Pharmacological Research 158 (2020) 104852

Contents lists available at ScienceDirect

Pharmacological Research

journal homepage: www.elsevier.com/locate/yphrs

A phytoestrogen secoisolariciresinol diglucoside induces browning of white adipose tissue and activates non-shivering thermogenesis through AMPK pathway

JongWook Kang[a,1], Jinbong Park[b,c,1], Woo Yong Park[a], Wenjun Jiao[a], Sujin Lee[a], Yunu Jung[b,c], Dong-Hyun Youn[b,c], Gahee Song[a], Seon Yeon Cho[a], Whi Young Kim[a], Ja Yeon Park[a], Kwang Seok Ahn[c], Hyun-Jeong Kwak[d], Jae-Young Um[b,c,*]

[a] Department of Science in Korean Medicine, Graduate School, Kyung Hee University, 26, Kyungheedare-ro, Dongdaemun-Gu, Seoul, 02447, Republic of Korea
[b] Department of Pharmacology, College of Korean Medicine, Kyung Hee University, 26, Kyungheedae-ro, Dongdaemun-Gu, Seoul, 02447, Republic of Korea
[c] Basic Research Laboratory for Comorbidity Regulation, Comorbidity Research Institute, Kyung Hee University, 26, Kyungheedae-ro, Dongdaemun-Gu, Seoul, 02447, Republic of Korea
[d] Major of Life Science, Division of Bioconvergence, College of Convergence and Integrated Science, Kyonggi University, 154-42 Gwanggosan-ro, Yeongtong-gu, Suwon-si, Gyeonggi-do 16227, Republic of Korea

ARTICLE INFO

Chemical compounds studied in this article:
Secoisolariciresinol diglucoside (SDG)
PubChem CID: 9917980

Keywords:
Secoisolariciresinol diglucoside
Obesity
Brown/Beige adipocytes
Thermogenesis
AMPKα
Mitochondria

ABSTRACT

Secoisolariciresinol diglucoside (SDG) is the main phytoestrogen component of flaxseed known as an antioxidant. Current study focused on the effect of SDG in white adipose tissue (WAT) browning. Browning of WAT is considered as a promising treatment strategy for metabolic diseases. To demonstrate the effect of SDG as an inducer of browning, brown adipocyte markers were investigated in inguinal WAT (iWAT) of high fat diet-fed obese mice and genetically obese *db/db* mice after SDG administration. SDG increased thermogenic factors such as uncoupling protein 1, peroxisome proliferator-activated receptor gamma coactivator 1 alpha and PR domain containing 16 in iWAT and brown adipose tissue (BAT) of mice. Similar results were shown in beige-induced 3T3-L1 adipocytes and primary cultured brown adipocytes. Furthermore, SDG increased factors of mitochondrial biogenesis and activation. We also observed SDG-induced alteration of AMP-activated protein kinase α (AMPKα). As AMPKα is closely related in the regulation of adipogenesis and thermogenesis, we then evaluated the effect of SDG in AMPKα-inhibited conditions. Genetic or chemical inhibition of AMPKα demonstrated that the role of SDG on browning and thermogenesis was dependent on AMPKα signaling. In conclusion, our data suggest SDG as a potential candidate for improvement of obesity and other metabolic disorders.

1. Introduction

Obesity, defined as BMI > 30, is a crucial health problem worldwide [1]. There are 1.5 billion individuals overweight and 500 million of these are considered obese, and this number is constantly increasing. Obesity affects the risk of hypertension, dyslipidemia, diabetes mellitus, therefore its impact on world health cannot be neglected [2,3]. However, the treatment for obesity and related metabolic diseases is still an

Abbreviations: ACC, acetyl-CoA carboxylase; ALT, alanine transaminase; AST, aspartate aminotransferase; ATGL, adipose triglyceride lipase; AMPK, AMP-activated protein kinase α: BAT, brown adipose tissue; C/EBPa, CCAAT/enhancer-binding protein a; CIDEA, cell death activator; COX-2, cyclooxygenase-2; COX4, cytochrome c oxidase subunit 4; COX8, cytochrome c oxidase subunit 8; CPT1, carnitine palmitoyltransferase 1; CytoC, cytochrome c; eWAT, epididymal white adipose tissue; FIS1, mitochondrial fission 1; GAPDH, glyceraldehyde-3-phosphate dehydrogenase; HDL, high density lipoprotein density lipoprotein; H&E, hematoxylin and eosin; HFD, high-fat diet; HSL, hormone-sensitive lipase; IF, immunofluorescence; iWAT, inguinal white adipose tissue; LDL, low density lipoprotein; LKB1, liver kinase B1; MFN1, mitofusin-1; MTS, 3-(4,5-dimethylthiazol-2-yl)-5-(3-carboxymethoxyphenyl)-2-(4-sulfophenyl)-2H-tetrazolium; ND, normal diet; NRF1, nuclear respiratory factor 1; OGTT, oral glucose tolerance test; PGC1a, peroxisome proliferator activated receptor g-coactivator 1-a; PPARg, peroxisome proliferator activated receptor g; PRDM16, PR domain containing 16; SCD1, stearoyl-CoA desaturase-1; SDG, secoisolariciresinol diglucoside; siRNA, small interfering RNA; SIRT3, sirtuin-3; SREBP1, sterol regulatory element-binding protein 1; TC, total cholesterol; TG, triglyceride; UCP1, uncoupling protein 1; WAT, white adipose tissue; WT, wild type

* Corresponding author.
E-mail address: jyum@khu.ac.kr (J.-Y. Um).
[1] These authors contributed equally to this work.

https://doi.org/10.1016/j.phrs.2020.104852
Received 19 November 2019; Received in revised form 30 March 2020; Accepted 20 April 2020
Available online 11 May 2020

unfinished business. There are only five available medications approved by the FDA, which limits the choice of practitioners and patients. Furthermore, the approved five medications: orlistat, phentermine-topiramate, lorcaserin hydrochlodride, naltrexone hydrochlodride-bupropion hydrochloride, and liraglutide all display side effects, some with can be potentially fatal [3,4]. Thus, the search for potential anti-obese agents is still necessary to develop an effective, yet safer treatments for obesity. In line, the potential of natural products is gaining interest [5,6]. Secoisolariciresinol diglucoside (SDG) is an antioxidant phytoestrogen [7], which is a main compound of lignin and present in flaxeed [8]. Flaxseeds belong to the phytoestrogen family, which are well known to benefit health, especially in cardiovascular diseases [9,10]. Our previous study has also shown the anti-adipogenic effect of SDG [11].

Obesity is caused by an imbalance between energy intake and expenditure. When the energy intake exceeds expenditure, the excessive energy is stored in the form of lipid [12]. Mammals have two types of adipose tissue; white adipose tissue (WAT) and brown adipose tissue (BAT). These two types of tissue have metabolically distinguished roles. The main role of WAT is storing excessive energy, while BAT displays a specific defense mechanism against cold called non-shivering thermogenesis. The non-shivering thermogenesis program can be induced not only by the cold but also by pharmacological or nutritional stimuli [13]. After recent studies have shown that adults possess considerably functional BAT [14], the thermogenic activation of BAT has a clinically important meaning because BAT contributes to a systemic increase of whole-body energy expenditure [15].

Similar thermogenic conditions in WAT are reported as well. Transdifferentiation of functional brown adipocytes, also termed as beige (or brite) adipocytes, can be induced from white adipocytes and display thermogenic potential. Although the origin of beige adipocytes differs from classical brown adipocytes, they share a large role in the differentiation process [16]. Activation of both brown and beige adipocytes is dependent on the increase of uncoupling protein 1 (UCP1) of which action occurs in the mitochondrial inner membrane. Inducing the mitochondrial UCP1 action can result in the activation of thermogenesis in BAT or WAT, thus is a possible strategy for obesity treatment [17].

AMP-activated protein kinase α (AMPK α) is the main regulator of the energy balance in the whole body. AMPK is in other words is a metabolic sensor, which responds to AMP/ATP ratio; if AMP is increased, AMPK activates to induce ATP production [18,19]. In this condition, catabolism (i.e. fatty acid oxidation) is increased and anabolism (i.e. fatty acid synthesis) is inhibited. Focusing on the role of AMPK and its upstream liver kinase B1 (LKB1) [20,21] and downstream target acetyl-CoA carboxylase (ACC) [22,23] is also a promising pathway for conquering obesity.

Our previous work demonstrated the beneficial effect of SDG in obesity by suppressing adipogenesis in high fat diet (HFD)-fed obese mice and 3T3-L1 adipocytes [11].

In this study, we reveal its effect on other potent mechanisms for obesity regulation. Herein, we use genetically obese *db/db* mice, HFD-induced obese mice and vitro models of brown and beige adipocytes to elucidate the role of SDG in thermogenesis more deeply.

2. Material and methods

2.1. Drugs and reagents

SDG, insulin, 3-isobutylmethylxanthine (IBMX), dexamethasone, indomethacin, 3,3,5-triiodo-L-thyronine (T3), and Oil Red O powder were purchased from Sigma Chemical Co. (St Louis, MO, USA) Dulbecco's modified Eagle's medium (DMEM), penicillin-streptomycin, bovine serum (BS), and fetal bovine serum (FBS) were from Gibco BRL (Grand Island, NY, USA).

2.2. Ethical statement

All animal experiments were performed in accordance with the ethical guidelines of Kyung Hee University and approved by the Institutional Review Board of Kyung Hee University (confirmation number: KHUASP (SE)-15-08).

2.3. Animal experiments

Animal experiments were performed as previously described [11,15]. Briefly, 5-week-old male *db/db* mice were purchased from Daehan Biolink (Eumsung, South Korea) and maintained for 1 week before the experiments. Then *db/db* Mice ($n \geq 5$) were orally administered with SDG prepared in distilled water (50 mg/kg) for 5 times per week while control *db/db* mice were administered with distilled water for 5 times per week as well.

Four-week-old male C57BL/6J mice ($n \geq 5$) were purchased from Daehan Biolink (Eumsung, South Korea) and maintained for 1 week before the experiments. To induce obesity, mice were fed a HFD for 4 weeks prior to SDG treatment. Then, the HFD-fed animals were randomly divided into two groups of five mice. The mice were fed for additional 12 weeks with a) HFD (60% kcal supplemented by fat) or b) HFD plus SDG (50 mg/kg of body weight/day). Normal chow diet was fed for 16 weeks to the normal control (NC) mice. The animals were given free access to food and tap water. Body weight and food intake were recorded every week. At the end of the period, the animals were fasted overnight, anesthetized under CO_2 asphyxiation. The CO_2 has displaced to the cage by 20% per minute. After the cage has been full of CO_2, mice were kept for 10 min for euthanasia.

Serum was separated immediately after blood collection by centrifugation at 400*g* for 30 min. Cardiac puncture was done after sacrifice using the KOVAX-Syringe 26 G (Korea Vaccine Co. LTD, Seoul, South Korea). The tissues were collected, placed in a tube, and stored at −80 °C.

2.4. Blood serum analysis

Serum total cholesterol (TC), low density lipoprotein (LDL)-cholesterol, high density lipoprotein (HDL)-cholesterol, triglyceride (TG), alanine transaminase (ALT), aspartate aminotransferase (AST), and creatinine were analyzed using enzymatic colorimetric methods by Seoul Medical Science Institute (Seoul Clinical Laboratories, Seoul, South Korea).

2.5. Hematoxylin & Eosin (H&E) staining and immunofluorescence assay

Histological analysis was performed as previously described [11,24]. Briefly, the tissues were fixed in 10% formalin and embedded in paraffin. The sections were stained with H&E staining and immunofluorescence assay. Microscopic examinations were performed and photographs were taken under a regular light microscope. Adipose tissues were analyzed in three randomly selected pictures. Immunofluorescence assays were done after fixation with 4% paraformaldehyde in PBS for 15 min. Then cells were permeabilized with 0.2% Triton X-100 (Sigma) for 10 min and thereafter, unspecific binding sites were blocked using PBS with 1% BSA (Calbiochem, La Jolla, CA). The antibodies against uncoupling protein 1 (UCP1) and peroxisome proliferator-activated receptor gamma coactivator 1-alpha (PGC1α) were purchased from Santa Cruz Biotechnology (Santa Cruz, CA, USA). UCP1 primary antibody was used at a dilution of 1:200 and incubated for 30 min. Alexa 594 (Invitrogen) was used as a secondary antibody at 1:500 and incubated for 1 h. PGC1α primary antibody was diluted in PBS with 1% BSA at the concentration of 1:200 and incubated for 1 h. Alexa 488 (Invitrogen) was used as a secondary antibody at 1:500 in PBS and incubated for 1 h. Fluorescence signals were imaged using a Zies LSM 5 Pascal laser confocal microscope (Carl Zeiss, Inc., Jena, Germany).

Table 1
Primer sequences used for real-time RT-PCR.

	Primer 5′–3′	
Target gene	Sense	Anti-sense
UCP1	AACTGTACAGCGGTCTGCCT	TAAGCCGGCTGAGATCTTGT
PGC1α	AATGCAGCGGTCTTAGCACT	TGTTGACAAATGCTCTTCGC
PGC1β	CGTATTTGAGGACAGCAGCA	TACTGGGTGGGCTCTGGTAG
Cidea	TGACATTCATGGGATTGCAGAC	GGCCAGTTGTGATGACTAAGAC
NRF1	CCACGTTGGATGAGTACACG	CAGACTCGAGGTCTTCCAGG
NRF2	CCGGAGACCCTTAGATCGA	TAGCCTGTAAAAGATTTCTGCAAACC
Tfam	ATTCCGAAGTGTTTTTCCAGCA	TCTGAAAGTTTTGCATCTGGGT
CPT1 α	GACTCCGCTCGCTCATTCC	GACTGTGAACTGGAAGGCCA
ATP5 α1	CTGTACTGCATCTACGTCGCGA	AGCCTGCTTGGATAGATCGTCATA
COX4i1	ATTGGCAAGAGAGCCATTTCTAC	TGGGGAAAGCATAGTCTTCACT
COX8b	TGTGGGGATCTCAGCCATAGT	AGTGGGCTAAGACCCATCCTG
ERRα	CTCAGCTCTCTACCCAAACGC	CCGCTTGGTGATCTCACACTC
FASN	AACGTCACTTCCAGCTAGAC	GTCCAGGCTGTGGTGACTCT
MCAD	CCAGAGAGGAGATTATCCCCG	TACACCCATACGCCAACTCTT
GAPDH	AACTTTGGCATTGTGGAAGG	GGATGCAGGGATGATGTTCT

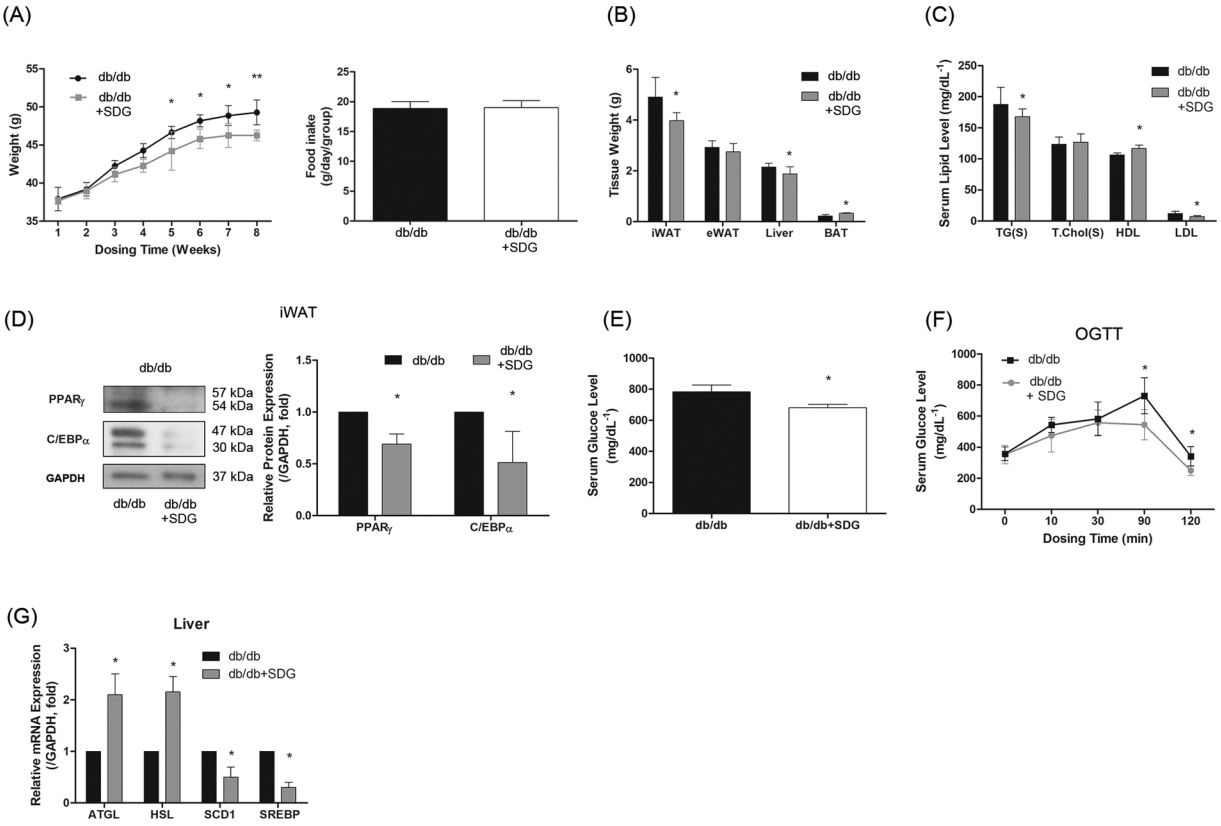

Fig. 1. Effect of SDG on obesity- and adipogenesis-related factors in *db/db* mice. Genetically obese *db/db* mice were administered SDG (50 mg/kg/day) for 8 weeks. (A) Changes in body weight (black square, *db/db* mice; gray square, *db/db* fed with SDG) and food intake (g/day/group) were measured. (B) Tissue weight of eWAT, iWAT, liver and BAT were measured. (C) Serum levels of triglyceride, total cholesterol, HDL cholesterol and LDL cholesterol were measured. (D) Protein expression levels of PPARγ and C/EBPα in iWAT were measured by a Western blot analysis. GAPDH was used as an endogenous control. (E) Serum level of glucose was measured after sacrifice. (F) Oral glucose tolerance test was performed and baseline serum glucose level was measured. (G) mRNA expression levels of *Atgl*, *Hsl*, *Scd1* and *Srebp* in liver were measured by a real-time RT-PCR analysis. *Gapd*h was used as an endogenous control. Data are expressed as the mean ± SEM of three or more experiments. Statistical analysis was done by the *t*-test to compare two groups. More than 2 groups were calculated by using the one-way ANOVA. $*p < 0.05$ vs. *db/db* mice, $**p < 0.01$ vs. *db/db* mice.

2.6. Glucose tolerance test

For an oral glucose tolerance test (OGTT), mice were orally administered glucose (2 g/kg of body weight) in sterilized water after fasting for 16 h. Blood glucose was measured from the tail (by removing the distal 2 mm of the tail) at 0, 10, 30, 90, and 120 min after delivering gavage, using a glucometer (Accu-Chek Performa device, Roche Diagnostics, Mannheim, Germany).

2.7. Cell isolation, culture and adipocyte differentiation

Brown adipocytes were obtained from interscapulum BAT of mice (postnatal 1–3 days) and isolated by collagenase dispersion. This dissection was performed as described by Klein *at al.* [25]. Beige

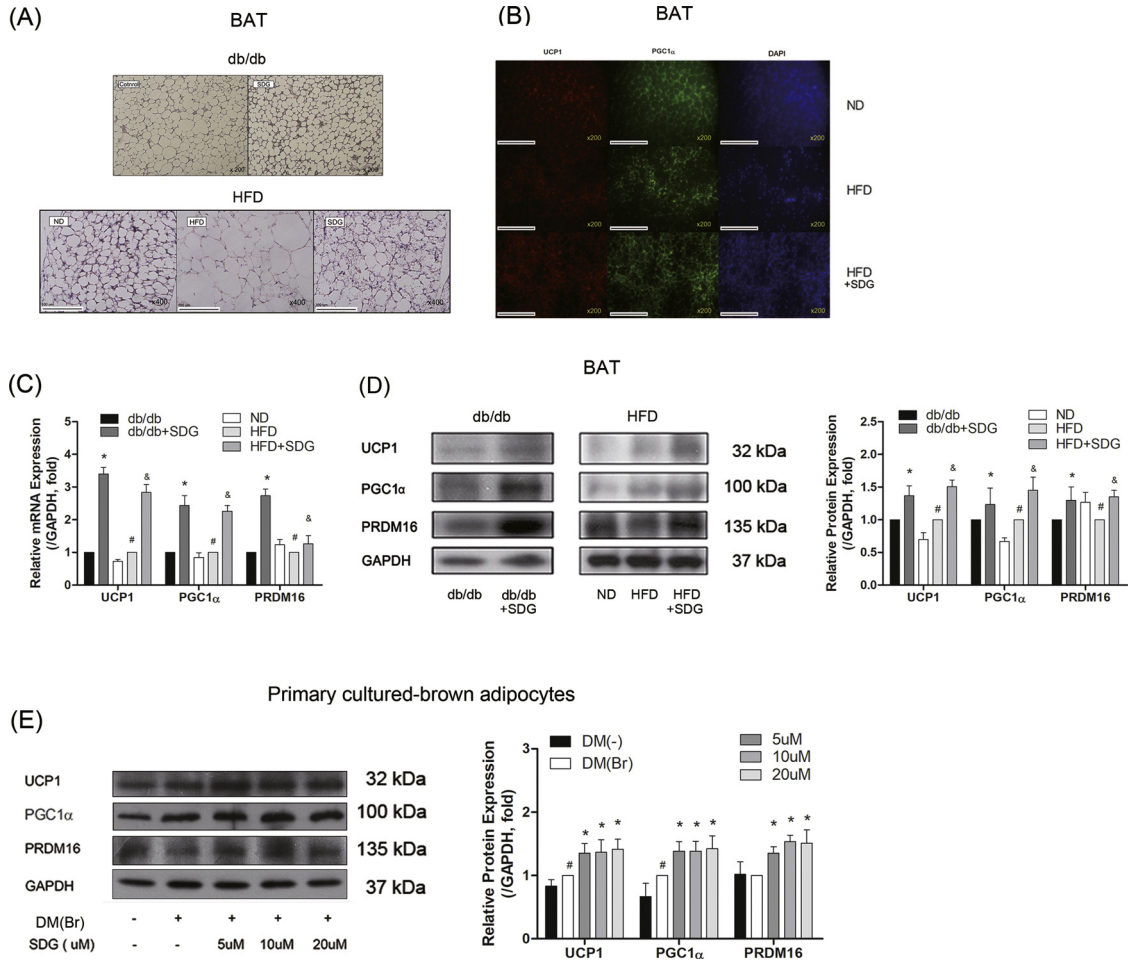

Fig. 2. Effect of SDG on thermogenesis-related factors in BAT and primary-cultured brown adipocytes. (A) Histological structure of BAT of *db/db* mice (upper panel, ×200) and HFD-fed C57BL/6 mice (lower panel, ×400) were observed after H&E staining. (B) IF staining of UCP1 (red) and PGC1α (green) in BAT of HFD-fed C57BL/6 mice was performed. (C) mRNA expression levels of *Ucp1*, *Pgc1a* and *Prdm16* in BAT were measured by a real-time RT-PCR analysis. *Gapdh* was used as an endogenous control. (D) Protein expression levels of UCP1, PGC1α and PRDM16 in BAT were measured by a Western blot analysis. (D) Protein expression levels of UCP1, PGC1α and PRDM16 in primary-cultured brown adipocytes were measured by a Western blot analysis. GAPDH was used as an endogenous control. Data are expressed as the mean ± SEM of three or more experiments. Statistical analysis was done by the *t*-test to compare two groups. More than 2 groups were calculated by using the one-way ANOVA. (C) and (D): $^{*}p < 0.05$ vs. *db/db* mice, $^{\#}p < 0.05$ vs. ND-fed mice, $^{\&}p < 0.05$ vs HFD-fed mice. (E): $^{\#}p < 0.05$ vs. undifferentiated preadipocytes, $^{*}p < 0.05$ vs. differentiated brown adipocytes. (For interpretation of the references to colour in this figure legend, the reader is referred to the web version of this article.)

adipocytes were differentiated from 3T3-L1 adipocytes (American Type Culture Collection, Rockville, MD, USA), passage number 10. Brown adipocytes [15], beige adipocytes and 3T3-L1 adipocytes [11] were differentiated as described previously. Briefly, cells were grown in DMEM plus 10% BS and plated for final differentiation in DMEM plus 10% FBS with 100 units/mL of penicillin streptomycin solution at 37 ˚C, in 5% CO_2, at 95% humidity until confluence. Two days after confluence (Day 0), the cells were stimulated to differentiate with differentiation inducers (White: 1 μM dexamethasone, 500 μM 3-isobutyl-1-methylxanthine and 1 μg/mL insulin; Beige: 1 μM dexamethasone, 500 μM 3-isobutyl-1-methylxanthine, 1 μg/mL insulin and 20 μM T3; Brown: 1 μM dexamethasone, 500 μM 3-isobutyl-1-methylxanthine, 1 μg/mL insulin, 20 μM T3 and 125 μM indomethacin) that were added to DMEM containing 10% FBS for two days (Day 2). Pre-adipocytes were then cultured in DMEM, 10% FBS supplemented with 1 μg/mL insulin for white adipocytes, 1 μg/mL insulin, 500 μM 3-isobutyl-1-methylxanthine, 20 μM T3 and 0.5 μM troglitazone for beige adipocytes, or 1 μg/mL insulin, 500 μM 3-isobutyl-1-methylxanthine, 20 μM T3 and 125 μM indomethacin for brown adipocytes for another two days (Day 4), followed by culturing with 10% FBS/DMEM medium for an additional two days (Day 6), at which time more than 90% of the cells were mature adipocytes with accumulated fat droplets.

2.8. Cell vitality assessment

Cell viability was measured with a cell proliferation 3-(4,5-dimethylthiazol-2-yl)-5-(3-carboxymethoxyphenyl)-2-(4-sulfophenyl)-2H-tetrazolium (MTS) kit (Promega, Madison, WI, USA) according to the manufacturer's instructions as previously described [11].

2.9. Oil-red O staining

Lipid accumulation in adipocytes was measured by an Oil-Red O staining assay as described previously [19]. The cells stained with Oil Red O solution were observed by an Olympus IX71 Research Inverted Phase microscope (Japan). The absorbance of the isopropanol-extracted dye was measured at 500 nm in a VERSA max microplate reader (Molecular Devices, Sunnyvale, CA, USA).

2.10. Western blot analysis

Western blotting for protein expression analysis was performed as

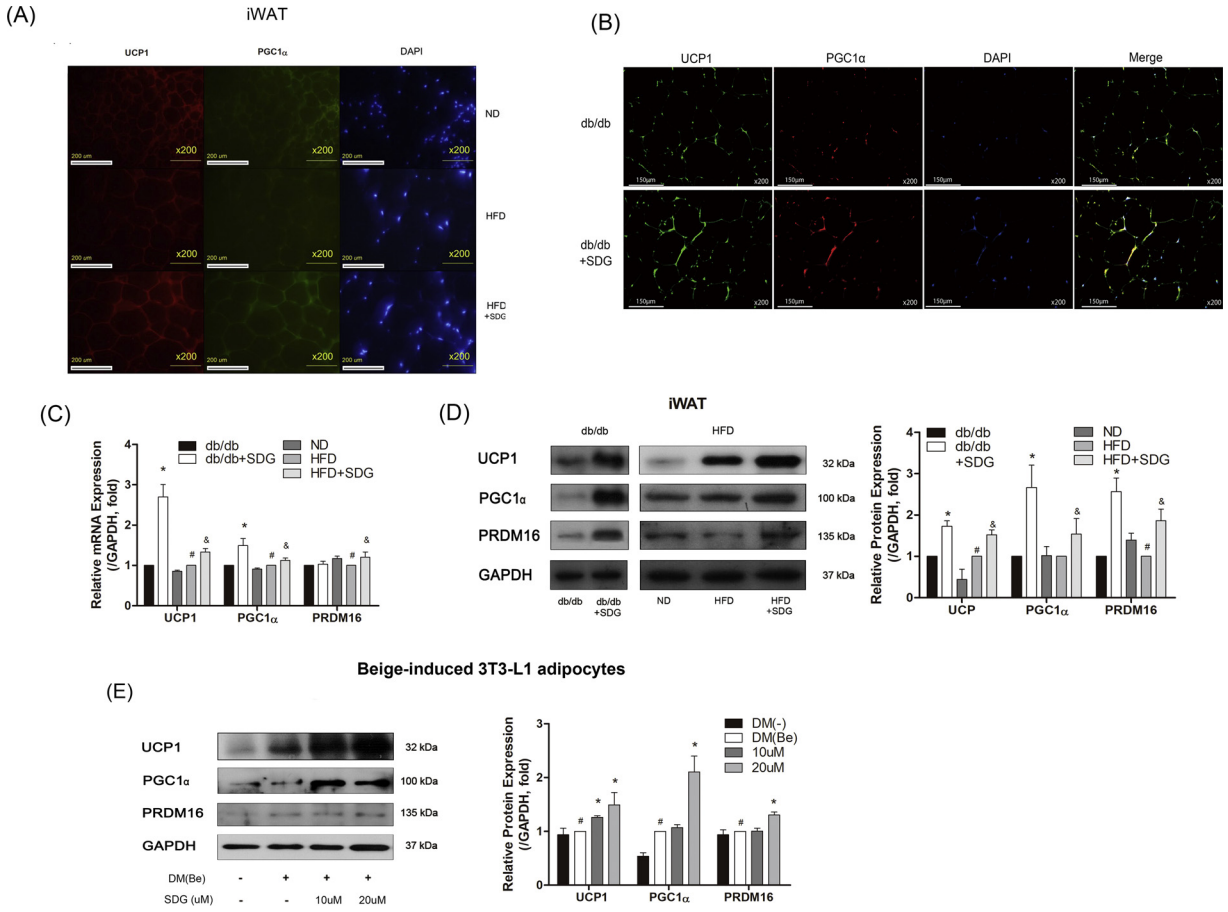

Fig. 3. Effect of SDG on beige-related factors in iWAT and beige-induced 3T3-L1 adipocytes. IF staining of UCP1 and PGC1α in iWAT of (A) HFD-fed C57BL/6 mice and (B) *db/db* mice (×200) was performed. (C) mRNA expression levels of *Ucp1*, *Pgc1a* and *Prdm16* in iWAT were measured by a real-time RT-PCR analysis. *Gapd*h was used as an endogenous control. (D) Protein expression levels of UCP1, PGC1α and PRDM16 in iWAT were measured by a Western blot analysis. (E) Protein expression levels of UCP1, PGC1α and PRDM16 in beige-induced 3T3-L1 adipocytes were measured by a Western blot analysis. GAPDH was used as an endogenous control. Data are expressed as the mean ± SEM of three or more experiments. Statistical analysis was done by the *t*-test to compare two groups. More than 2 groups were calculated by using the one-way ANOVA. (C) and (D): $^{*}p < 0.05$ vs. *db/db* mice, $^{\#}p < 0.05$ vs. ND-fed mice, $^{\&}p < 0.05$ vs HFD-fed mice. (E): $^{\#}p < 0.05$ vs. undifferentiated preadipocytes, $^{*}p < 0.05$ vs. beige-induced 3T3-L1 adipocytes.

previously described [11]. Anti-UCP1, anti-PGC1α, anti−CCAAT/enhancer-binding protein alpha (C/EBPα), anti-mitochondrial fission 1 protein (FIS1), anti- mitofusin-1 (MFN1) and anti-glyceraldehyde-3-phosphate dehydrogenase (GAPDH) were purchased from Santa Cruz Biotechnology (Santa Cruz, CA, USA). Anti-peroxisome proliferator-activated receptor gamma (PPARγ), anti-nuclear respiratory factor 1 (NRF1), anti-phospho liver kinase B1 (LKB1), anti-LKB1, anti-phospho AMP-activated protein kinase α (AMPKα), anti-AMPKα, anti-phopho acetyl-CoA carboxylase (ACC) and anti-ACC antibodies were purchased from Cell Signaling Technology (Beverly, MA, USA). Anti-PR domain containing 16 (PRDM16), Anti-cell death activator (CIDEA) and anti-cytochrome C were purchased from Abcam (Cambridge, United Kingdom).

2.11. RNA extraction and real-time PCR

RNA extraction and real-time PCR were performed as in a previous report [23]. Briefly, RNA extraction was performed using a GeneAllR RiboEx total RNA extraction kit (GeneAll Biotechnology, Seoul, Korea), cDNA reverse transcription was performed using a Power cDNA synthesis kit (iNtRON Biotechnology, Seongnam, Kyunggi, Korea), and the real-time PCR was performed by a Step One Real-Time PCR System (Applied Biosystems, Foster City, CA, USA). The primers used in this study are shown in Table 1.

2.12. AMPK siRNA transfection

The transfection of siRNAs was performed according to our previous study [11]. First, siRNA transfection was carried out 2 days after the confluence of pre-adipocytes. Lipofectamine 2000 (5 μL) and 10 μL siRNA (10 pmol) were individually diluted and incubated in 250 μL Opti-MEM medium (Invitrogen, Carlsbad, CA, USA) for 20 min. Then, they were mixed and incubated for 30 min before being added to each well. The initial medium was removed and replaced with induction medium 48 h after transfection.

2.13. Mitochondrial microscopic analysis

MitoTracker staining and observation was performed as described previously [15] using a MitoTracker Red probes CM-XRos (Invitrogen, Carlsbad, CA, USA).

2.14. Oxygen consumption analysis

Oxygen consumption in cells were measured by a Mito-ID Extracellular O_2 sensor kit (Enzo Life Science, ENZ-51045, USA) according to the instruction provided by the manufacturer. Briefly, O_2 sensor probe (10 μl) was added into beige-induced 3T3-L1 adipocytes or primary cultured brown adipocyte treated with 0, 10 and 20 μM of SDG. After covering with 2 drops (about 100 μl) of Mito-ID HS Oil, the plates

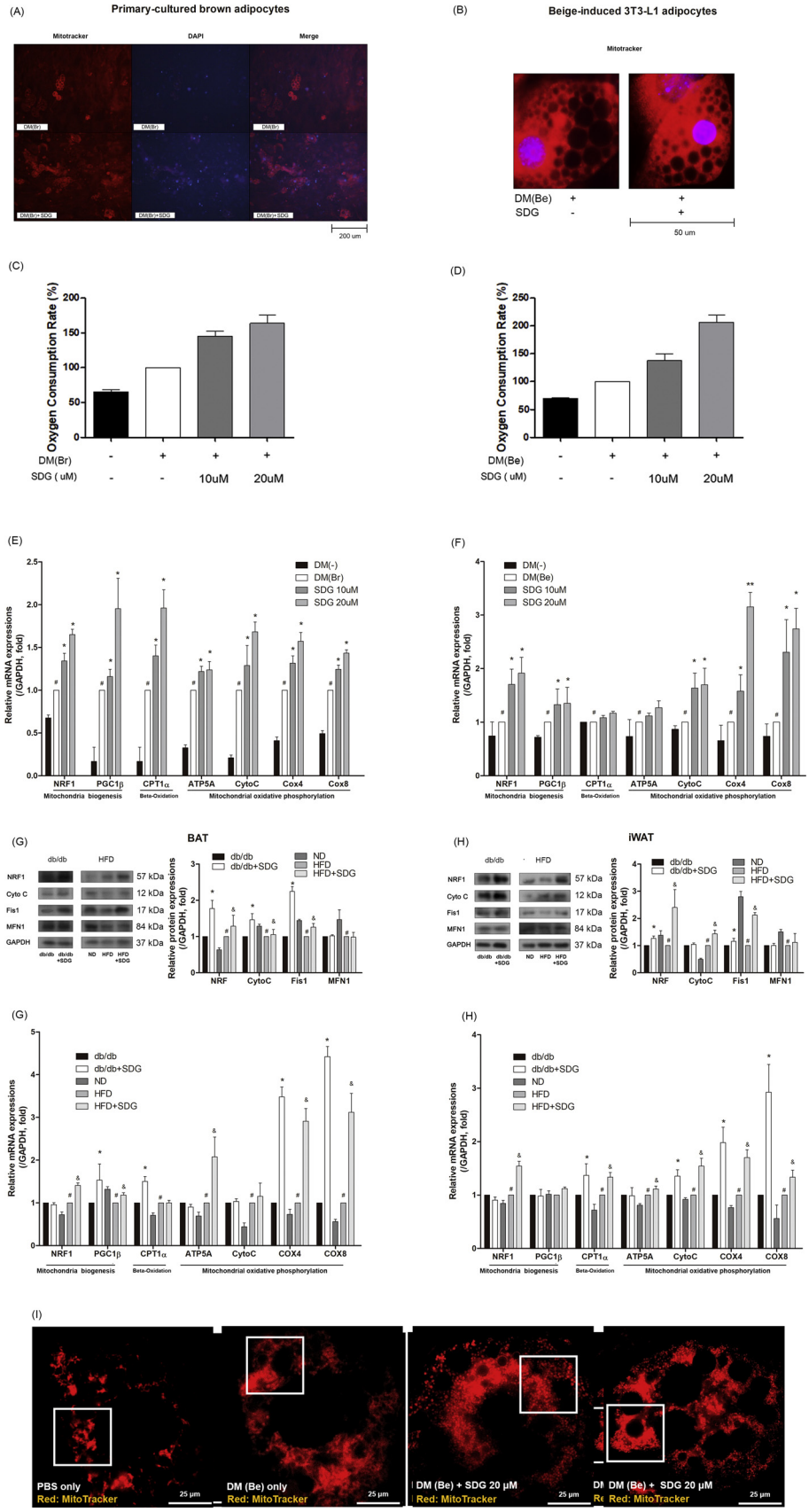

Fig. 4. Effect of SDG on mitochondrial biogenesis and activation in vivo and in vitro. Mitochondrial abundance was analyzed in (A) primary-cultured brown adipocytes and (B) beige-induced 3T3-L1 adipocytes by MitoTracker Red staining. Oxygen consumption rate was measured in (C) primary-cultured brown adipocytes and (D) beige-induced 3T3-L1 adipocytes. mRNA levels of genes related in mitochondrial biogenesis (*Nrf1* and *Pgc1b*), Beta-oxidation (*Cpt1a*) and mitochondrial oxidative phosphorylation (*Atp5a*, *CytoC*, *Cox4il* and *Cox8b*) were analyzed in (E) primary-cultured brown adipocytes and (F) beige-induced 3T3-L1 adipocytes by real-time RT-PCR analyses. *Gapd*h was used as an endogenous control. Protein levels of NRF1, Cytochrome C, FIS1 and MFN1 were measured in (G) BAT and (H) iWAT of *db/db* and HFD-fed mice by Western blot analyses. GAPDH was used as an endogenous control. mRNA levels of genes related in mitochondrial biogenesis (*Nrf1* and *Pgc1b*), Beta-oxidation (*Cpt1a*) and mitochondrial oxidative phosphorylation (*Atp5a*, *CytoC*, *Cox4il* and *Cox8b*) were analyzed in (G) BAT and (H) iWAT of *db/db* and HFD-fed mice by real-time RT-PCR analyses. *Gapd*h was used as an endogenous control. (I) MitoTracker staining was performed to evaluate mitochondrial dynamics. Data are expressed as the mean ± SEM of three or more experiments. Statistical analysis was done by the *t*-test to compare two groups. More than 2 groups were calculated by using the one-way ANOVA. (C)-(F): $^{\#}p < 0.05$ vs. undifferentiated preadipocytes, $^{*}p < 0.05$ vs. differentiated adipocytes, $^{**}p < 0.01$ vs. differentiated adipocytes. (G) and (H): $^{*}p < 0.05$ vs. *db/db* mice, $^{\#}p < 0.05$ vs. ND-fed mice, $^{\&}p < 0.05$ vs HFD-fed mice.

were read of 380 nm for excitation and 650 nm of emission at 30 ˚C. The measured values were normalized to count cell nuclear by DAPI. The absorbance was measured in a VARIOSKAN LUX spectrophotometer (Thermo Fischer Scientific, Vantaa, Finland).

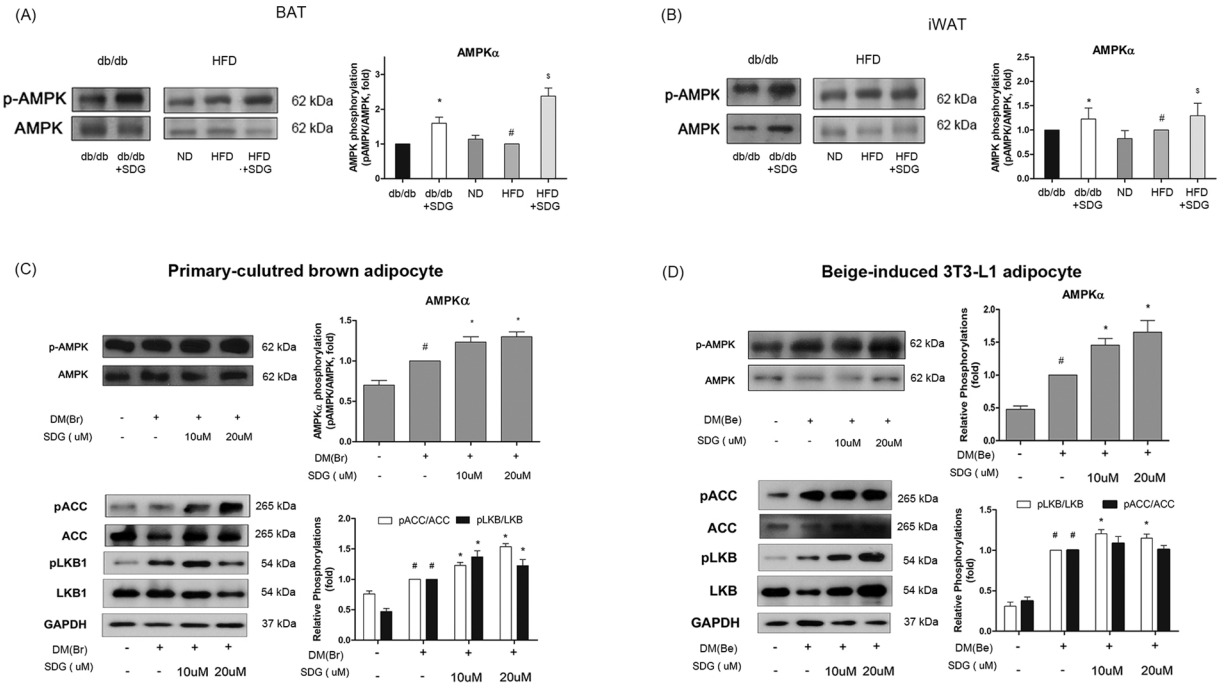

Fig. 5. Effect of SDG on LKB1-AMPKα-ACC pathway in vivo and in vitro. Phosphorylation level of AMPKα in (A) BAT and (B) iWAT of *db/db* and HFD-fed mice was measured by a Western blot analysis. Phosphorylation levels of AMPKα, ACC and LKB1 in (C) primary-cultured brown adipocytes and (D) beige-induced 3T3-L1 adipocytes were measured by Western blot analyses. GAPDH was used as an endogenous control. pAMPKα, pACC and pLKB1 expressions were normalized against AMPKα, ACC and LKB1 expressions respectively. Data are expressed as the mean ± SEM of three or more experiments. Statistical analysis was done by the *t*-test to compare two groups. More than 2 groups were calculated by using the one-way ANOVA. (A) and (B): $^{*}p < 0.05$ vs. *db/db* mice, $^{\#}p < 0.05$ vs. ND-fed mice, $^{\&}p < 0.05$ vs HFD-fed mice. (C) and (D): $^{\#}p < 0.05$ vs. undifferentiated preadipocytes. $^{*}p < 0.05$ vs. differentiated adipocytes.

2.15. Statistical analysis

All data were expressed as mean ± standard error mean (SEM) of three or more experiments. Statistical significance ($p < 0.05$) was calculated using the Mann–Whitney non-parametric analysis of Student's *t*-test to compare two groups and more 3 groups for Windows (SPSS Inc., Chicago, IL, USA).

3. Results

3.1. SDG alleviates obesity-related symptoms in db/db mice and HFD-fed obese mice

We have demonstrated the anti-obesity effects of SDG in our previous study [11]. By in vitro studies using 3T3-L1 adipocytes and in vivo studies of HFD-induced obesity in mice, we could confirm its anti-obesity effect via inhibition of adipogenesis of white adipocytes. In the current study, we attempt to examine the thermogenic effects of SDG. First, in Fig. 1A, concomitantly to our previous results, we found that the SDG treatment group showed a significant reduction in weight gain in *db/db* mice with no significant difference in food intake. To provide further evidence supporting the beneficial effect of SDG, we measured the weight of BAT, inguinal WAT, epididymal WAT and liver tissue (Fig. 1B). SDG treatment reduced the weight of liver tissue and inguinal WAT of *db/db* mice ($p < 0.05$). By analyzing serum, we confirmed increased HDL-cholesterol and reduced LDL-cholesterol levels, indicating improved lipid metabolism by SDG treatment (Fig. 1C). Triglyceride level was also reduced by SDG treatment with significant differences ($p < 0.05$). However, total cholesterol did not show a significant difference between SDG-treated mice and vehicle-treated mice. Similar results were observed in HFD-fed obese C57BL/6J mice (Supplementary Fig. S1A and B). SDG treatment suppressed body weight gain and improved serum lipid profiles.

Next, we investigated whether SDG can regulate major adipogenesis factors including PPARγ and C/EBPα [26], reveal the mechanism of WAT decrease in *db/db* mice (Fig. 1 D). As expected, and also in line with our previous study [11], SDG indeed inhibited the protein expressions of both regulators of adipogenesis.

As in Fig. 1E, the basal serum glucose level was reduced by SDG treatment when measured in serum collected from cardiac puncture after sacrifice. Fig. 1F further shows that SDG improved the glucose metabolism induced by an OGTT, implying that SDG treatment leads to a significant enhancement in glucose sensitivity.

These results demonstrate that SDG inhibits obesity by decreasing the adipogenesis in HFD and *db/db* mice.

3.2. SDG attenuates HFD-induced hepatic steatosis

Pathogenic accumulation of lipid within the liver tissue, also known as hepatic steatosis, is another obesity-related symptom [27]. Thus, we investigated whether SDG could improve such phenomenon in *db/db* mice. Since increase of liver-related enzymes such as alanine aminotransferase (ALT) and aspartate aminotransferase (AST) are commonly observed in hepatic steatosis, we have investigated the effect of SDG on these enzymes. As shown in Fig. S2, SDG treatment significantly reduced both AST and ALT in *db/db* mice and HFD mice. Furthermore, lipogenic markers including stearoyl-CoA desaturase-1 (SCD1) and sterol regulatory element-binding protein 1 (SREBP1) [28,29] were decreased, while lipolytic markers including ATGL and HSL were increased by SDG treatment (Fig. 1G). These results indicate that SDG alleviates hepatic steatosis by reducing lipogenesis and inducing lipolysis, and thus the liver tissue weight is decreased.

3.3. SDG induces non-shivering thermogenesis of brown adipocytes in vivo and in vitro

Activation of non-shivering thermogenesis is an additional mechanism which may participate in obesity treatment by inducing weight

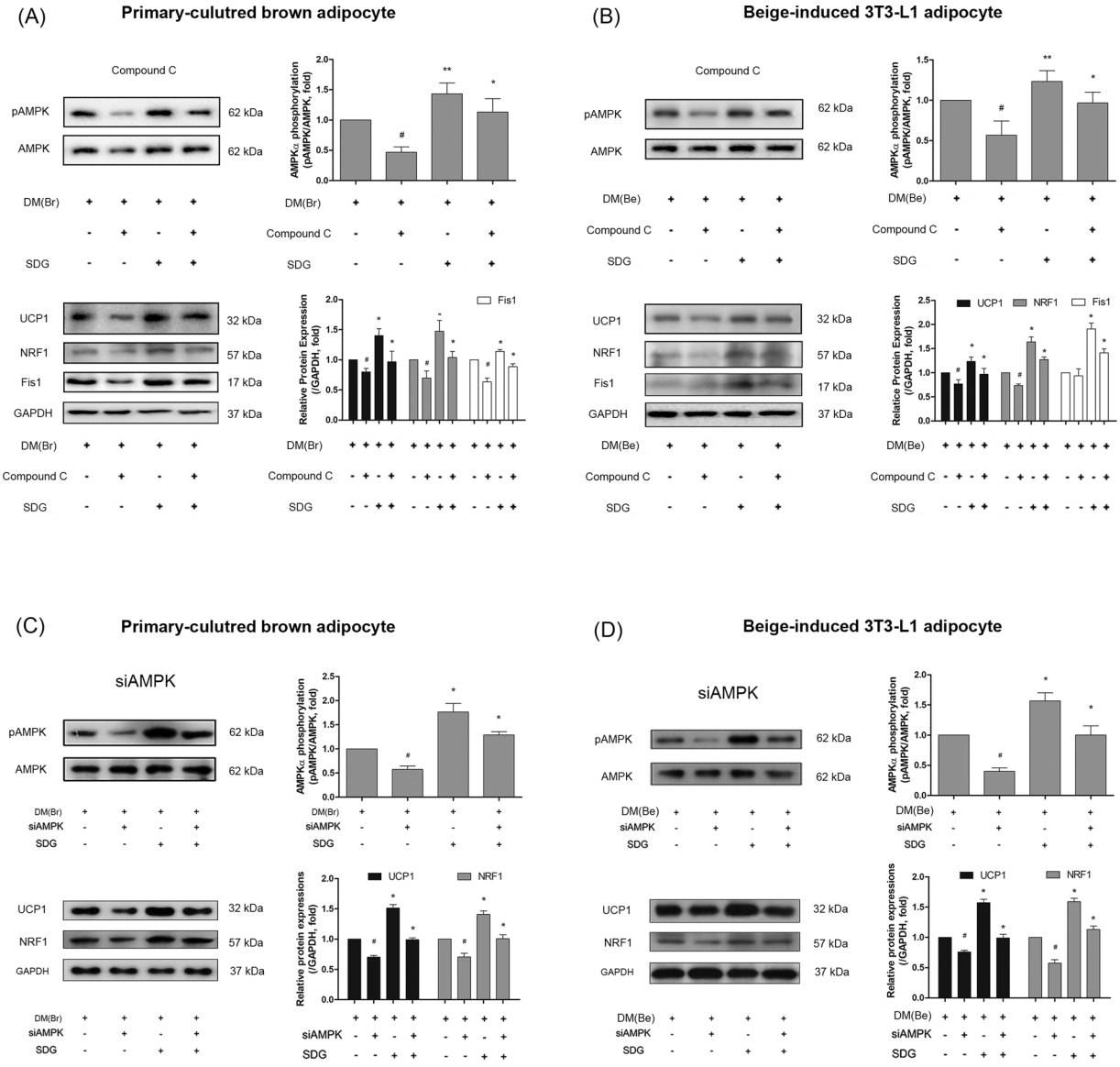

Fig. 6. Effect of SDG on thermogenesis- and mitochondria-related factors in AMPKα-inhibited conditions. Protein expressions of pAMPKα, UCP1, NRF1 and FIS1 were measured after pre-treatment with a potent AMPKα inhibitor Compound C in (A) primary-cultured brown adipocytes and (B) beige-induced 3T3-L1 adipocytes by Western blot analyses. Protein expressions of AMPKα, UCP1 and NRF1 were measured after pre-treatment with siAMPKα in (C) primary-cultured brown adipocytes and (D) beige-induced 3T3-L1 adipocytes by Western blot analyses. GAPDH was used as an endogenous control. pAMPKα expression was normalized against AMPKα expression. DW was used as vehicle. Data are expressed as the mean ± SEM of three or more experiments. Statistical analysis was done by the *t*-test to compare two groups. More than 2 groups were calculated by using the one-way ANOVA. $^{*}p < 0.05$ vs. compound C-treated adipocytes. (C) and (D): $^{\#}p < 0.05$ vs. vehicle-treated adipocytes, $^{*}p < 0.05$ vs. siAMPKα-treated adipocytes.

loss. To confirm the effects of SDG in such context, we examined the effects of SDG on BAT-related thermogenesis. First, we observed the change in histological aspects by staining BAT with hematoxylin and eosin (H&E). As a result, SDG-treated mice showed reduced size of lipid droplets when compared to mice of the control group (Fig. 2A).

Further IF staining showed the increase of key thermogenesis factors including UCP1 and PGC1α in the BAT tissue was induced by SDG (Fig. 2B). To confirm, Western blot analysis and real-time RT-PCR analysis were carried out to measure thermogenesis factors at the protein and mRNA levels. Both protein and mRNA expressions of UCP1 (and its gene *Ucp1*) and PGC1α (and its gene *Pgc1a*) were increased in the BAT of SDG-treated *db/db* and HFD mice (Fig. 2C and D) mice. ($^{*}p$ = in *db/db* mice; $^{\&}p$ = in SDG vs HFD-fed mice; $^{\#}p$ = in ND vs HFD-fed mice).

To find out if the effect of SDG affects BAT activation in a cell autonomous manner, in vitro experiments were performed in primary cultured brown adipocytes. First, we confirmed the cytotoxicity of SDG in primary cultured brown adipocytes, of which results showed that SDG had no significant cytotoxicity up to the concentration of 50 μM (Supplementary Fig. S3). However, an Oil-Red O staining experiment revealed that 50 μM of SDG negatively affected development of brown adipocytes (Supplementary Fig. S4). Therefore, the final concentrations of SDG used in following experiments were fixed as 5, 10, and 20 μM. By performing a Western blot assay in SDG-treated primary brown adipocytes, we could observe similar results to the ones from in vivo experiments: UCP1, PGC1α and PRDM16 was increased by SDG treatment (Fig. 2E).

3.4. SDG activates browning of white adipocytes in vivo and in vitro

As we had confirmed the thermogenic effect of SDG in BAT, our next goal was to find out if it could affect the trans-differentiation of white

adipocytes into beige adipocytes, the potential next-generation-strategy for obesity care. To clarify, we confirmed the thermogenesis factors in WAT and beige-induced 3T3-L1 adipocytes. First, we analyzed the expression and location of two thermogenic proteins, UCP1 and PGC1α by IF staining, and could observe a massive increase in both factors (Fig. 3A). Similar results were observed in iWAT of *db/db* mice as well (Fig. 3B). Furthermore, both protein and mRNA expressions of UCP1, PGC1α and PRDM16 were significantly increased in the SDG-treated groups compared with vehicle-treated *db/db* mice or HFD-fed mice (Fig. 3C and D).

To confirm, we established a beige adipocyte model by treating troglitazone in 3T3-L1 adipocytes based on a previous report [30,31].In this cell line of beige adipocyte, SDG was able to increase factors related in transdifferentiation and activation of beige adipocytes including UCP1, PGC1, and PRDM16 as well (Fig. 3E).

3.5. SDG induces mitochondrial biogenesis and activation in brown and beige adipocytes in vivo and in vitro

To investigate the detailed pathway in SDG-related thermogenesis, we observed the change in mitochondria-related factors induced by SDG. First, to investigate the effect of SDG on mitochondrial development and activation during the differentiation of brown adipocytes, a MitoTracker staining was performed in primary cultured brown adipocytes. SDG-treated brown adipocytes displayed enhanced signals of mitochondria. On Day 8, the final day of differentiation, SDG treatment showed higher IF signals associated with lipid accumulation, indicating the promotion of brown adipocyte development (Fig. 4A). Similar enhancement of mitochondrial signaling was shown in beige-induced 3T3-L1 adipocytes (Fig. 4B). Oxygen consumption rate (OCR) was also measured after SDG treatment. As a result, SDG significantly increased OCR in both primary cultured brown adipocytes (Fig. 4C) and beige-induced 3T3-L1 adipocytes (Fig. 4D).

Next, we investigated whether mitochondrial factors were affected by SDG treatment. By a real-time RT-PCR analysis, genes related in mitochondrial biogenesis (*Tfam*), mitochondrial activation (*Nrf1, Pgc1b*) and mitochondrial β oxidation (*Cpt1a, Atp5a, Cox4il, Cox8b*) were measured, showing the SDG-induced alteration of these majority of these mitochondrial genes in primary-cultured brown adipocytes and beige-induced 3T3-L1 adipocytes (Fig. 4E and F).

NRF1 and Cytochrome C are well-known factors in the biogenesis and activation of mitochondria [32]. As shown in Fig. 4E and F, NRF1 was increased with a significant difference in both BAT and iWAT of SDG-treated *db/db* mice and HFD-fed obese mice. However, Cytochrome C showed a slight increase by SDG treatment, but did not display significant difference with vehicle-fed mice ($^{*}p$ = in *db/db* mice; $^{\&}p$ = in SDG vs. HFD-fed mice, $^{\#}p$ = in ND vs. HFD-fed mice). In additional mRNA analyses, levels of *Tfam*, *Nrf1, Pgc1bCpt1a, Atp5a, Cox4il* and *Cox8b* were validated in adipose tissues of SDG-treated mice (Fig. 4G and H). As a result, significant up-regulation of *Pgc1b*, *Cpt1a*, *Cox4il* and *Cox8* was observed in SDG-treated *db/db* mice, while increase of *Nrf1*, *Atp5a*, *Cox4il* and *Cox8* was induced by SDG in HFD-fed obese mice.

Mitochondrial fusion and fission, the dynamics of mitochondria, dramatically occur during activation of non-shivering thermogenesis [33]. The change in MFN1, the fusion marker of mitochondria, and Fis1, the fission marker of mitochondria [34,35], were observed to verify the effect of SDG on mitochondria dynamics. As a result, we could observe that only fission increased in SDG-treated conditions, while the fusion marker MFN1 showed a tendency to decrease (Fig. 4G and H). In addition, by staining SDG-treated cells with MitoTracker, we could observe the dividing forms of mitochondria, implying increased fission by SDG (Fig. 4I). From these results, we demonstrated that one of the pathways of SDG is mitochondria activation of thermogenesis.

3.6. SDG activates phosphorylation of LKB1-AMPKα-ACC axis in brown and beige adipocytes in vivo and in vitro

In our previous study [11], we reported that SDG activated AMPKα and consequently inhibited adipogenesis of white adipocytes. Based on this previous observation, we investigated whether AMPKα also has a role in the SDG-induced thermogenesis. First, we measured the expression of AMPK in vivo. In BAT and iWAT of both *db/db* and HFD-fed obese mice, AMPKα was increased by SDG treatment (Fig. 5A and B).

As described previously, the metabolic sensor AMPKα responds to low metabolic status to expend energy [22]. During this process, not only this single protein, but also others related in the AMPK pathway are changed as well. The upstream factor of AMPK, LKB1, and the downstream target of AMPK, ACC, are also phosphorylated while AMPK is activated. In primary cultured brown adipocytes, we confirmed that phosphorylation of LKB and ACC was increased by SDG treatment (Fig. 5C). In addition, beige-induced 3T3-L1 adipocytes treated with SDG displayed similar results, however, without statistical significance in ACC phosphorylation ($p = 0.05$) (Fig. 5D).

3.7. Thermogenic activation of SDG is dependent on AMPKα activation

To reveal the underlying mechanism of the effect of SDG, we created an AMPK-inhibited condition by blocking the activation of AMPK with compound C, a widely used AMPK inhibitor [36]. As shown in Fig. 6A, compound C pre-treatment decreased phosphorylation of AMPKα. In such an environment of suppressed AMPK activation, SDG treatment failed to induce thermogenic activation or mitochondrial activation/dynamics, when confirmed by a Western blot analysis of UCP1, NRF1 and FIS1. This result was observed in both primary cultured brown adipocytes and beige-induced 3T3-L1 adipocytes (Fig. 6A and B).

To confirm, we next treated brown and beige adipocytes with siRNA treatment to disturb transcription of AMPK. AMPK siRNA was added to the culture medium prior to SDG treatment and blocked the expression of AMPK effectively (Fig. 6C and D, upper panels). In primary cultured brown adipocytes and beige-induced 3T3-L1 adipocytes, SDG administration in siAMPK-treated cells failed to increase either UCP1 or NRF1, in line with the results from pharmacological inhibited conditions (Fig. 6C and D, lower panels).

4. Discussion

Obesity is a metabolic disease, which results from energy imbalance: the difference between energy intake and expenditure [37]. There have been many attempts to conquer obesity; however, an effective therapy with no side effects has yet to be developed. Our previous study showed the potential of SDG an effective anti-obesity agent via suppressing adipogenesis through regulation of the AMPKα pathway [38,39]. In this study, we assessed the anti-obese effect of SDG in the concept of non-shivering thermogenesis. Non-shivering thermogenesis, originally a defense mechanism against cold, is a rising strategy for obesity care [40]. First, to verify whether SDG actually does display anti-obesity effects by suppressing body weight gain, we used genetically obese *db/db* mice and HFD-induced obese mice. SDG reduced the weight gain of mice separate from their food intake, improved the lipid profile within serum. Well-known obesity markers PPARγ and C/EBPα were also decreased by SDG treatment in iWAT of *db/db* mice consistent with our previous report [11]. Serum analysis determined the beneficial effect of SDG on lipid profiles including HDL-cholesterol and LDL-cholesterol within serum, and furthermore, through an OGTT assessment, we could observe SDG positively regulated glucose sensitivity.

Hepatic steatosis, especially nonalcoholic fatty liver disease (NAFLD), is closely related to obesity. Although not all obese individuals have hepatic steatosis, a retrospective study by Gaba et al. [41] reported liver steatosis is present in nearly 50% (18 of 39 patients) of overweight individuals and nearly 70% (38 of 57 patients) in obese

individuals. Enzymes indicating hepatotoxicity; AST and ALT, are also frequently altered in serum of hepatic steatosis patients [42,43]. In this study, SDG-treated mice displayed lower AST and ALT serum levels compared to vehicle-treated control mice. Beneficial changes were induced by SDG in factors of lipogenesis and lipolysis in liver tissue as well. From these results we could think that SDG improves not only adiposity but also obesity-related abnormal hepatic lipid accumulation.

The development and activation of brown adipocytes within BAT is well-established since its rediscovery in 2009 [44]. Not solely BAT, but also the recruitment of functionally thermogenic beige adipocytes within WAT has gained interest since its first observational report as well [45]. PGC1α promotes UCP1 to activate thermogenesis in these two distinct types of adipocytes [46], while PRDM16 has a role during differentiation of brown adipocytes, and also plays a crucial role during the trans-differentiation of white adipocytes into beige adipocytes [19]. Our results obviously show that SDG treatment induces the thermogenic program in brown/beige adipocytes in vivo and in vitro. UCP1, PGC1α and PRDM16 expressions were elevated by SDG treatment in BAT and primary cultured brown adipocytes. In addition, in iWAT of *db/db* mice and beige-induced 3T3-L1 adipocytes, SDG significantly increased these crucial factors in development and activation of functional thermogenic adipocytes. Furthermore, oxygen consumption rate was increased in both brown and beige adipocytes by SDG treatment. In short, we had found that SDG induces the development and activation of brown fat, and moreover, can increase the thermogenic capacity in white fat as well.

Cytochrome C, NRF1 and Carnitine palmitoyltransferase 1 alpha (CPT1α) are known as enzymes responsible for mitochondrial respiration and oxidation [47]. In addition, cytochrome c oxidase subunit 4 (COX4) and cytochrome c oxidase subunit 8 (COX8) are located in the mitochondria inner membrane and directly regulate the electronic transfer chain [48]. Mitochondrial dynamics is also known to participate in the activation of thermogenic adipocytes [33]. Mitochondrial fission factor FIS1 and the mediator of mitochondrial fusion MFN1 are mitochondrial membrane proteins that interact with each other to facilitate mitochondrial dynamics during cold-induced thermogenesis [49]. Our results on these factors demonstrated that SDG can significantly induce mitochondrial biogenesis, activation and fission. NRF1, required for mitochondrial respiration [50], was increased by SDG treatment. MFN1, the fusion promoter was not affected, but FIS1, the essential regulator of mitochondrial fission was increased in SDG-treated brown/beige adipocytes. Increase in COX4 and COX8, the cytochrome c oxidase subunits which contributes to mitochondrial electron transport, can be used as indicators of mitochondria count and activity [51–53]. Our study found that SDG treatment increased *Cox4il* and *Cox8b*, the genes which transcript the two subunits respectively. Since increased mitochondria abundance is also a main characteristic of brown adipocyte and beige adipocytes, we specifically stained mitochondria using the MitoTracker stain to find out SDG increased the expression of mitochondria in both primary-cultured brown adipocytes and beige-induced 3T3-L1 adipocytes. These results showed that SDG can induce mitochondrial biogenesis and stimulate mitochondrial activation of β oxidation and fission.

Although UCP1 act as the main factor in non-shivering thermogenesis, this whole program is also regulated by the AMPK pathway, the sensor and regulator of energy homeostasis [54]. As we revealed the AMPK-activating action of SDG in our previous report [11], we evaluated its role in the thermogenic effect of SDG as well. We confirmed LKB1-AMPK-ACC pathway was phosphorylated in brown and beige fat by SDG treatment. By assessing the effect of SDG in further investigations using pharmacological inhibitor or siRNA for AMPKα, we could confirm that the role of AMPKα is crucial for SDG to activate the thermogenic potential in both brown and beige adipocytes.

In conclusion, we verify that SDG has an anti-obesity effect by increasing AMPKα pathway and thus activating non-shivering thermogenesis and stimulating mitochondrial biogenesis/activation/fission. From these results, we demonstrate that SDG, a natural product derived from flaxseed, can be a safe yet effective therapeutic agent for metabolic disorders including obesity.

Author contributions

J. Kang and J. Park performed most of the experiments and contributed to data interpretation; W.Y. Park, W. Jiao, S. Lee, Y. Jung, D.H. Youn, S.Y. Cho, W.Y. Kim, G. Song, J.Y. Park, K.S. Ahn and H.J. Kwak assisted with methodology; J. Kang, J. Park, W.Y. Park and W. Jiao curated data; J.Y. Um gathered resources; J. Kang, J. Park and J.Y. Um conceived and designed the experiments and wrote the manuscript; J.Y. Um acquired funding; J.Y. Um supervised the project; and all authors read and approved the manuscript.

Acknowledgements

This work was supported by the National Research Foundation of Korea (NRF) grant funded by the Korea government (MSIP) (NRF-2015R1A4A1042399 and 2017M3A9E4065333).

Appendix A. Supplementary data

Supplementary material related to this article can be found, in the online version, at doi:https://doi.org/10.1016/j.phrs.2020.104852.

References

[1] K.M. Flegal, M.D. Carroll, C.L. Ogden, L.R. Curtin, Prevalence and trends in obesity among US adults, 1999-2008, JAMA 303 (2010) 235–241.
[2] R.S.L. Cassani, P.G. Fassini, J.H. Silvah, C.M.M. Lima, J.S. Marchini, Impact of weight loss diet associated with flaxseed on inflammatory markers in men with cardiovascular risk factors: a clinical study, Nutr. J. 14 (2015) 5.
[3] H.L. Daneschvar, M.D. Aronson, G.W. Smetana, FDA-approved anti-obesity drugs in the United States, Am. J. Med. 129 (879) (2016) e1 879. e6.
[4] A.J. Krentz, K. Fujioka, M. Hompesch, Evolution of pharmacological obesity treatments: focus on adverse side-effect profiles, Diabetes Obes. Metab. 18 (2016) 558–570.
[5] N. Vasudeva, N. Yadav, S.K. Sharma, Natural products: a safest approach for obesity, Chin. J. Integr. Med. 18 (2012) 473–480.
[6] C. Fu, Y. Jiang, J. Guo, Z. Su, Natural products with anti-obesity effects and different mechanisms of action, J. Agric. Food Chem. 64 (2016) 9571–9585.
[7] J.L. Adolphe, S.J. Whiting, B.H. Juurlink, L.U. Thorpe, J. Alcorn, Health effects with consumption of the flax lignan secoisolariciresinol diglucoside, Br. J. Nutr. 103 (2010) 929–938.
[8] C. Strandås, A. Kamal-Eldin, R. Andersson, P. Åman, Phenolic glucosides in bread containing flaxseed, Food Chem. 110 (2008) 997–999.
[9] K. Prasad, Secoisolariciresinol diglucoside from flaxseed delays the development of type 2 diabetes in Zucker rat, J. Lab. Clin. Med. 138 (2001) 32–39.
[10] S. Bashir, S. Ali, F. Khan, Partial reversal of obesity-induced insulin resistance owing to anti-inflammatory immunomodulatory potential of flaxseed oil, Immunol. Invest. 44 (2015) 451–469.
[11] J. Kang, J. Park, H. Kim, Y. Jung, D. Youn, S. Lim, et al., Secoisolariciresinol diglucoside inhibits adipogenesis through the Ampk pathway, Eur. J. Pharmacol. 820 (2018) 235–244.
[12] P. Poirier, T.D. Giles, G.A. Bray, Y. Hong, J.S. Stern, F.X. Pi-Sunyer, et al., Obesity and cardiovascular disease: pathophysiology, evaluation, and effect of weight loss: an update of the 1997 American Heart Association Scientific Statement on Obesity and Heart Disease from the Obesity Committee of the Council on Nutrition, Physical Activity, and Metabolism, Circulation 113 (2006) 898–918.
[13] D. Berryman, E. List, Growth hormone's effect on adipose tissue: quality versus quantity, Int. J. Mol. Sci. 18 (2017) 1621.
[14] Lichtenbelt van Marken, D. Wouter, J.W. Vanhommerig, N.M. Smulders, J.M. Drossaerts, G.J. Kemerink, N.D. Bouvy, et al., Cold-activated brown adipose tissue in healthy men, N. Engl. J. Med. 360 (2009) 1500–1508.
[15] Y. Jung, J. Park, H. Kim, J. Sim, D. Youn, J. Kang, et al., Vanillic acid attenuates obesity via activation of the AMPK pathway and thermogenic factors in vivo and in vitro, FASEB J. 32 (2017) 1388–1402.
[16] K. Ikeda, P. Maretich, S. Kajimura, The common and distinct features of brown and beige adipocytes, Trends Endocrinol. Metab. 29 (2018) 191–200.
[17] H. Kim, J. Park, H. Park, Y. Jung, D. Youn, J. Kang, et al., Platycodon grandiflorum A. De Candolle ethanolic extract inhibits adipogenic regulators in 3T3-L1 cells and induces mitochondrial biogenesis in primary brown preadipocytes, J. Agric. Food Chem. 63 (2015) 7721–7730.
[18] S. Bijland, S.J. Mancini, I.P. Salt, Role of AMP-activated protein kinase in adipose tissue metabolism and inflammation, Clin. Sci. 124 (2013) 491–507.
[19] M. Jeong, H. Kim, J. Park, Y. Jung, D. Youn, J. Lee, et al., Rubi Fructus (Rubus

coreanus) activates the expression of thermogenic genes in vivo and in vitro, Int. J. Obes. 39 (2015) 456–464.
[20] A. Woods, S.R. Johnstone, K. Dickerson, F.C. Leiper, L.G. Fryer, D. Neumann, et al., LKB1 is the upstream kinase in the AMP-activated protein kinase cascade, Curr. Biol. 13 (2003) 2004–2008.
[21] S.A. Hawley, D.A. Pan, K.J. Mustard, L. Ross, J. Bain, A.M. Edelman, et al., Calmodulin-dependent protein kinase kinase-β is an alternative upstream kinase for AMP-activated protein kinase, Cell Metab. 2 (2005) 9–19.
[22] M. Foretz, D. Carling, C. Guichard, P. Ferre, F. Foufelle, AMP-activated protein kinase inhibits the glucose-activated expression of fatty acid synthase gene in rat hepatocytes, J. Biol. Chem. 273 (1998) 14767–14771.
[23] A. Woods, D. Azzout-Marniche, M. Foretz, S.C. Stein, P. Lemarchand, P. Ferré, et al., Characterization of the role of AMP-activated protein kinase in the regulation of glucose-activated gene expression using constitutively active and dominant negative forms of the kinase, Mol. Cell. Biol. 20 (2000) 6704–6711.
[24] J. Kang, G.H. Lee, Y. Jung, D.H. Youn, S. Lim, J. Park, et al., Igongsan reduces testosterone-induced benign prostate hyperplasia by regulating 5α-reductase in rats, Mol. Cell. Toxicol. 14 (2018) 211–220.
[25] J. Klein, M. Fasshauer, M. Ito, B.B. Lowell, M. Benito, C.R. Kahn, Beta(3)-Adrenergic stimulation differentially inhibits insulin signaling and decreases insulin-induced glucose uptake in brown adipocytes, J. Biol. Chem. 274 (1999) 34795–34802.
[26] M.I. Lefterova, Y. Zhang, D.J. Steger, M. Schupp, J. Schug, A. Cristancho, et al., PPARgamma and C/EBP factors orchestrate adipocyte biology via adjacent binding on a genome-wide scale, Genes Dev. 22 (2008) 2941–2952.
[27] E. Fabbrini, S. Sullivan, S. Klein, Obesity and nonalcoholic fatty liver disease: biochemical, metabolic, and clinical implications, Hepatology 51 (2010) 679–689.
[28] R. Ruiz, V. Jideonwo, M. Ahn, S. Surendran, V.S. Tagliabracci, Y. Hou, et al., Sterol regulatory element-binding protein-1 (SREBP-1) is required to regulate glycogen synthesis and gluconeogenic gene expression in mouse liver, J. Biol. Chem. 289 (2014) 5510–5517.
[29] H. Sampath, M. Miyazaki, A. Dobrzyn, J.M. Ntambi, Stearoyl-CoA desaturase-1 mediates the pro-lipogenic effects of dietary saturated fat, J. Biol. Chem. 282 (2007) 2483–2493.
[30] V. Krishnan, P. Baskaran, B. Thyagarajan, Troglitazone activates TRPV1 and causes deacetylation of PPARγ in 3T3-L1 cells, Biochimica et Biophysica Acta (BBA)-Molecular Basis of Disease 1865 (2019) 445–453.
[31] H. Ohno, K. Shinoda, B.M. Spiegelman, S. Kajimura, PPARγ agonists induce a white-to-brown fat conversion through stabilization of PRDM16 protein, Cell Metab. 15 (2012) 395–404.
[32] T.N. Tarasenko, S.E. Pacheco, M.K. Koenig, J. Gomez-Rodriguez, S.M. Kapnick, F. Diaz, et al., Cytochrome c oxidase activity is a metabolic checkpoint that regulates cell fate decisions during T cell activation and differentiation, Cell Metab. 25 (2017) 1254 1268. e7.
[33] T. Wai, T. Langer, Mitochondrial dynamics and metabolic regulation, Trends Endocrinol. Metab. 27 (2016) 105–117.
[34] D. Stojanovski, O.S. Koutsopoulos, K. Okamoto, M.T. Ryan, Levels of human Fis1 at the mitochondrial outer membrane regulate mitochondrial morphology, J. Cell. Sci. 117 (2004) 1201–1210.
[35] H. Chen, S.A. Detmer, A.J. Ewald, E.E. Griffin, S.E. Fraser, D.C. Chan, Mitofusins Mfn1 and Mfn2 coordinately regulate mitochondrial fusion and are essential for embryonic development, J. Cell Biol. 160 (2003) 189–200.
[36] X. Liu, R.R. Chhipa, I. Nakano, B. Dasgupta, The AMPK inhibitor compound C is a potent AMPK-independent antiglioma agent, Mol. Cancer Ther. 13 (2014) 596–605.
[37] E.Z. Amri, C. Dani, A. Doglio, J. Etienne, P. Grimaldi, G. Ailhaud, Adipose cell differentiation: evidence for a two-step process in the polyamine-dependent Ob1754 clonal line, Biochem. J. 238 (1986) 115–122.
[38] H.S. Moon, C.S. Chung, H.G. Lee, T.G. Kim, Y.J. Choi, C.S. Cho, Inhibitory effect of (-)-epigallocatechin-3-gallate on lipid accumulation of 3T3-L1 cells, Obesity Silver Spring (Silver Spring) 15 (2007) 2571–2582.
[39] S. Chen, P. Zhu, H. Guo, R.S. Solis, Y. Wang, Y. Ma, et al., Alpha1 catalytic subunit of AMPK modulates contractile function of cardiomyocytes through phosphorylation of troponin I, Life Sci. 98 (2014) 75–82.
[40] R. Calvani, C. Leeuwenburgh, E. Marzetti, Brown adipose tissue and the cold war against obesity, Diabetes 63 (2014) 3998–4000.
[41] R.C. Gaba, M.G. Knuttinen, T.R. Brodsky, S. Constantine, B.O. Omene, C.A. Owens, et al., Hepatic steatosis: correlations of body mass index, CT fat measurements, and liver density with biopsy results, Diagn. Interv. Radiol. 18 (2012) 282.
[42] R. Barcelos, S. Stefanello, J. Mauriz, J. Gonzalez-Gallego, F. Soares, Creatine and the liver: metabolism and possible interactions, Mini Rev. Med. Chem. 16 (2016) 12–18.
[43] E.G. Giannini, R. Testa, V. Savarino, Liver enzyme alteration: a guide for clinicians, CMAJ 172 (2005) 367–379.
[44] Lichtenbelt van Marken, D. Wouter, J.W. Vanhommerig, N.M. Smulders, J.M. Drossaerts, G.J. Kemerink, N.D. Bouvy, et al., Cold-activated brown adipose tissue in healthy men, N. Engl. J. Med. 360 (2009) 1500–1508.
[45] B. Cousin, S. Cinti, M. Morroni, S. Raimbault, D. Ricquier, L. Penicaud, et al., Occurrence of brown adipocytes in rat white adipose tissue: molecular and morphological characterization, J. Cell. Sci. 103 (Pt 4) (1992) 931–942.
[46] M.P. Cooper, M. Uldry, S. Kajimura, Z. Arany, B.M. Spiegelman, Modulation of PGC-1 coactivator pathways in brown fat differentiation through LRP130, J. Biol. Chem. 283 (2008) 31960–31967.
[47] K.L. Townsend, D. An, M.D. Lynes, T.L. Huang, H. Zhang, L.J. Goodyear, et al., Increased mitochondrial activity in BMP7-treated brown adipocytes, due to increased CPT1-anD. CD36-mediated fatty acid uptake, Antioxid. Redox Signal. 19 (2013) 243–257.
[48] F. Fontanesi, I.C. Soto, A. Barrientos, Cytochrome c oxidase biogenesis: new levels of regulation, IUBMB Life 60 (2008) 557–568.
[49] A. Hall, N. Burke, R. Dongworth, D. Hausenloy, Mitochondrial fusion and fission proteins: novel therapeutic targets for combating cardiovascular disease, Br. J. Pharmacol. 171 (2014) 1890–1906.
[50] H. Wu, S.B. Kanatous, F.A. Thurmond, T. Gallardo, E. Isotani, R. Bassel-Duby, et al., Regulation of mitochondrial biogenesis in skeletal muscle by CaMK, Science 296 (2002) 349–352.
[51] S. Altshuler-Keylin, K. Shinoda, Y. Hasegawa, K. Ikeda, H. Hong, Q. Kang, et al., Beige adipocyte maintenance is regulated by autophagy-induced mitochondrial clearance, Cell Metab. 24 (2016) 402–419.
[52] S. Kim, H. Kwon, S. Im, Y. Son, S. Akindehin, Y. Jung, et al., Connexin 43 is required for the maintenance of mitochondrial integrity in brown adipose tissue, Sci. Rep. 7 (2017) 7159.
[53] B. Van der Schueren, R. Vangoitsenhoven, B. Geeraert, D. De Keyzer, M. Hulsmans, M. Lannoo, et al., Low cytochrome oxidase 4I1 links mitochondrial dysfunction to obesity and type 2 diabetes in humans and mice, Int. J. Obes. 39 (2015) 1254.
[54] N. Kim, M. Nam, M.S. Kang, J.O. Lee, Y.W. Lee, G. Hwang, et al., Piperine regulates UCP1 through the AMPK pathway by generating intracellular lactate production in muscle cells, Sci. Rep. 7 (2017) 41066.